

Photodissociation Dynamics of Cyanamide at 212 nm

Chan Ho Kwon, Ji Hye Lee, and Hong Lae Kim*

Department of Chemistry, College of Natural Sciences, Kangwon National University, Chuncheon 200-701, Korea

*E-mail: hlkim@kangwon.ac.kr

Received May 30, 2007

Photodissociation dynamics of cyanamide (NH_2CN) at 212 nm has been investigated by measuring rotationally resolved laser induced fluorescence spectra of CN fragments exclusively produced in the ground electronic state. From the spectra, rotational population distributions of CN as well as translational energy releases in the products were obtained. The measured average rotational energies of CN were 12.4 ± 0.5 and 11.6 ± 0.5 kJ/mol for $v'' = 0$ and $v'' = 1$, respectively and the center of mass average translational energy release among products was 41.8 ± 6.4 kJ/mol. The observed energy partitioning was well represented by statistical prior calculations, from which it was suggested that the dissociation takes place on the ground electronic surface after rapid internal conversion.

Key Words : Photodissociation dynamics, Cyanamide, Laser induced fluorescence

Introduction

Gaseous cyanamide (NH_2CN) was identified in the interstellar cloud by detecting emission from the $4_{13} - 3_{12}$ and $5_{14} - 4_{13}$ rotational transitions in the microwave region.¹ Microwave and high resolution Fourier Transform Infrared spectra of cyanamide in the gas phase were extensively studied, from which the pyramidal structure about the amino nitrogen was determined together with theoretical investigations.²⁻⁶ In the gas phase, cyanamide is in equilibrium with carbodiimide that is a condensing agent able to induce the formation of peptides from amino acids.^{7,8} The isomerization of cyanamide into carbodiimide was observed either when cyanamide was condensed at low temperature (80 K) on an amorphous water ice surface as catalyst or by VUV irradiation at low temperature (10 K) in Ar or water matrix, and solid films.^{9,10} Considering the surface of cold dust grains in the interstellar cloud mainly consists of amorphous water ice, this catalytic isomerization reaction of cyanamide may be one of the origins of formation of biomolecular substances.

Photochemistry and photophysics of cyanamide in the gas phase is of considerable interest because it is a prebiotic molecule. In RCN molecules, a simple bond fission producing CN radicals was observed upon UV irradiation.¹¹⁻¹⁸ The lowest electronic transition in UV is mainly assigned as the $n \rightarrow \pi^*$ electronic transition, from which the dissociation takes places either on the excited state *via* predissociation or on the ground state *via* internal conversion. Mechanism of photodissociation of molecules could mainly be categorized as three: (1) direct dissociation on a repulsive excited electronic state, (2) predissociation resulting from couplings between excited states, and (3) dissociation on the ground state after internal conversion. In each case, the energy partitioning among degrees of freedom of the products, internal and translational, should be distinctive although it is complicated according to the manner of potential couplings

in the case (2). However, simple models can be applied to predict the energy partitioning for the case (1) and (3) such as an impulsive model and a statistical model, respectively. Since the dissociation dynamics should be governed by the nature of the electronic transition and by the shape of the potential energy surfaces leading to the individual product channels, the physical processes in the excited states can be investigated by studying the photodissociation dynamics.

In this report, a rotationally resolved laser induced fluorescence spectrum of CN produced from photodissociation of cyanamide at 212 nm was observed. From the spectrum, energy partitioning among the products was measured and the dissociation mechanism was discussed.

Experiments

The experiments were performed in a flow cell with conventional pump-probe geometry. The cell was evacuated at a pressure of 10^{-3} Torr with a mechanical pump. The solid sample of cyanamide was heated and the vapor of liquid (mp: 45 °C) at 60 °C was slowly flowed through the cell at a pressure of about 100 mTorr, which was controlled by needle valves. The stated purity of 99% of solid cyanamide was purchased from Aldrich and used without further purification.

The photolysis light at 212 nm was generated by frequency tripling of an output of a dye laser at 636 nm (Continuum ND-6000) pumped by the second harmonic of an Nd:YAG laser (Continuum, Surelite III). The dye laser output was introduced to a DKDP crystal for frequency doubling and the fundamental and doubled outputs were introduced to a BBO crystal through a half-wave plate to match the polarization. The efficiency of tripling was about 5% of the fundamental. The photolysis light beam was shaped as a circle (~ 3 mm dia. and ~ 5 mJ/cm²) with baffles that were placed inside arms attached to the cell. The baffles also minimized the scattered radiation into the detector. The

probe light to measure laser induced fluorescence spectra of CN at 389-382 nm employing $\tilde{B}-\tilde{X}$ transition was an output of a dye laser (HD-500, Lumonics) pumped by the third harmonic of an Nd:YAG laser (YM-800, Lumonics). The power of the probe light was kept as low as possible to avoid saturation in the spectra, which was typically about 30 $\mu\text{J}/\text{pulse}$ (~ 3 mm dia.). The LIF signal vs. photolysis laser power showed linear dependence up to 10 mJ/cm^2 , which ensured one-photon dissociation at the typical power used. The fluorescence signal was detected with a photomultiplier tube (1P28A, Hamamatsu) perpendicularly mounted relative to the laser beams through cut-off filters to reduce scattered radiation of the photolysis light. The measured signal was fed to a digital storage oscilloscope and integrated fluorescence signals were recorded. The delay between the pump and probe, typically about 100 ns was controlled with a digital pulse and delay generator. The sample pressure of 100 mTorr and the 100 ns delay time should provide a nascent product energy distribution. The measured fluorescence spectra were corrected with variation of the pump and probe laser powers and stored in a PC.

The laser line profile was measured from the rotational line profile of CN after translational relaxation by collisions. A Doppler line profile of one of the low N rotational transitions was measured at 2 μsec pump-probe delay with 5 Torr Ar, from which the laser line profile was measured after deconvolution of a Gaussian Doppler profile of CN at 300 K assuming complete relaxation. The estimated FWHM of the Lorentzian laser line profile was 0.27 cm^{-1} .

Results and Discussion

The LIF spectrum of CN ($\tilde{X}^2\Sigma, v'', N$) produced from photodissociation of cyanamide at 212 nm employing the $\tilde{B}^2\Sigma \leftarrow \tilde{X}^2\Sigma$ electronic transition is presented in Figure 1. In the spectra, the P branch bandheads of the 0-0 and 1-1 vibrational transitions clearly appear and the assignments for the R-branch rotational transitions are given on top of the

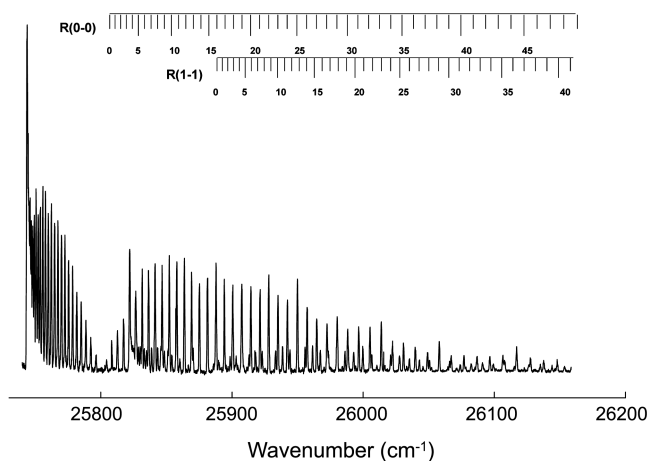


Figure 1. Laser induced fluorescence spectrum of CN produced from photodissociation of cyanamide at 212 nm employing the $\tilde{B}-\tilde{X}$ electronic transition.

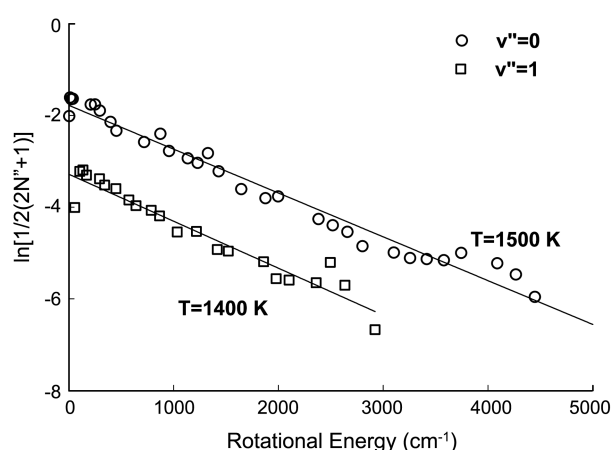


Figure 2. Boltzmann plots of rotational energy distribution of CN obtained from Figure 1.

spectra.¹⁹ The LIF signal in the region of 2-2 vibrational transition was negligibly small compared to the noise in the spectra, from which no population in $v'' = 2$ is assumed. The individual transitions would result from excitations of pairs of the spin doublets corresponding to $J = N \pm 1/2$ in these spectra according to the Hund case (b) electronic and rotational angular momentum couplings. The rotational population distributions were obtained from integrated intensities of the peaks corrected by appropriate line strength factors that are proportional to the square of the electronic transition moment, the Franck-Condon factors, and the Hönl-London factors, $2(N+1)$ in this case.²⁰ The average rotational energies of CN were then obtained from linear slopes of the Boltzmann plots, which were 12.4 ± 0.5 and $11.6 \pm 0.5 \text{ kJ/mol}$ for $v'' = 0$ and $v'' = 1$, respectively (Fig. 2). In addition, vibrational population distribution was obtained from the integrated intensities of the peaks from the 0-0 and 1-1 rovibrational transitions employing the reported Franck-Condon factors,²¹ which is 0.81/0.19 for $v'' = 0/1$.

The Doppler profiles of the individual rotational transi-

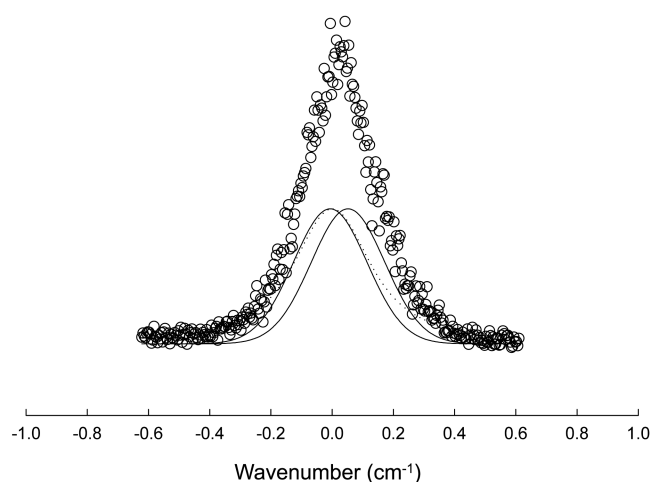


Figure 3. Doppler profile of the $R_{0,0}(4)$ rotational transition of CN. The dotted line is the laser line profile and the solid lines are the actual Doppler profiles after deconvolution of the laser line profile.

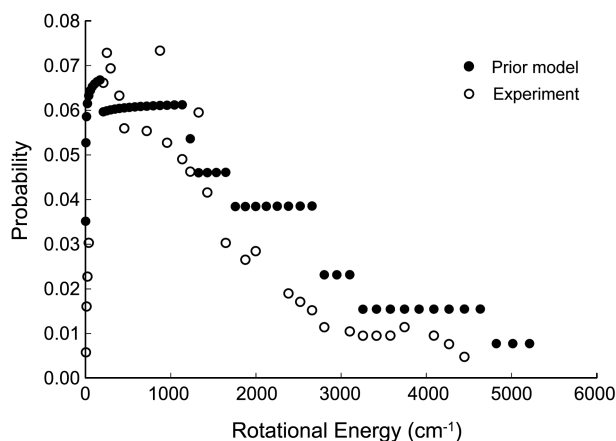


Figure 4. Rotational population distribution of CN at $v'' = 0$ obtained from the experiment (open circles) and the statistical prior calculations (closed circles).

tions in the spectra were analyzed to measure translational energies of the fragments. In Figure 3, the Doppler broadened spectra for $N = 4$ in the R branch rotational transitions are presented. The rotational transitions from the two spin doublet states were nearly overlapped at low N and almost resolved at high N under the given resolution of our laser. Since the separation of the two transitions at $N = 4$ is 0.06 cm^{-1} , the measured profile was estimated as the sum of the two transitions with Gaussian profiles, assuming isotropic velocity distribution for CN. Then, the actual Gaussian Doppler profiles were extracted by deconvolution of the measured laser line profile. The average translational energy of CN at $v'' = 0$ and $N = 4$ was measured from the second moment of the profile obtained from the best fit and then the center of mass translational energy release in the products was calculated to be $41.8 \pm 6.4 \text{ kJ/mol}$.

The reaction energy was obtained by the enthalpies of formation of NH_2CN , NH_2 and CN from literatures,^{22,23} which is 490.1 kJ/mol . Then, the calculated available energy for energy partitioning in the products, the photon energy at 212 nm minus the dissociation energy, was calculated to be 75.9 kJ/mol .

In order to figure out the dissociation mechanism, we applied the impulsive model and the statistical prior model to predict the rotational and translational energies of the products. Upon the electronic transition, the impulsive model assumes an abrupt turn-on of the repulsive force between atoms of the breaking bond, which results in large translational energy release in the products and then the internal energy distribution of the polyatomic products is developed afterwards.²⁴ Invoking linear and angular momentum conservation, the average translational and rotational energy of CN was calculated assuming the pyramidal structure obtained by ab initio molecular orbital calculations at the MP2/6-311++G** level using the GAUSSIAN 03 package of programs.²⁵ The calculated center of mass translational energy release and the rotational energy of CN were 51.8 and 17.2 kJ/mol , respectively, which are significantly different from the measured values. For the other extreme

Table 1. Energy partitioning (kJ/mol) among products produced from photodissociation of cyanamide at 212 nm

	E_{av}	$\langle E_t \rangle$	$\langle E_r \rangle$
	75.9		
Experiment		12.4 ± 0.5	41.8 ± 6.4
Prior		13.0	37.4
Impulsive		17.2	51.8

case, the energy partitioning was calculated using the prior model assuming slow dissociation on the vibrationally hot ground electronic state after the internal conversion.^{26,27} In this case, the available energy should be distributed among all product degrees of freedom with equal probability. Thus, the population of the individual rotational state of CN is proportional to the number of accessible quantum states in NH_2 at the energy $E = E_{av} - E_{CN}(v, J)$. The number of vibrational states, all possible overtones and combinations, was directly counted from fundamental vibrational frequencies obtained from the literature.²⁸ The calculated rotational distribution fits well to the observed distribution with minor deviation (Fig. 4) but the calculated average rotational energy of 13.0 kJ/mol agrees very well with the measurements. Similarly, the predicted average translational energy release from the same prior calculation was 37.4 kJ/mol , which again agrees well with the experiment (Table 1).

We concluded that the photodissociation of NH_2CN upon electronic absorption at 212 nm takes place on the ground electronic state after internal conversion resulting in statistical energy partitioning among the products. The minor deviation of the calculated rotational distribution from the observed should originate from incomplete randomization of the internal energy due to smallness of the molecular size and hence sparse vibrational states. The intramolecular vibrational energy randomization has almost always been observed in large polyatomic molecules with low frequency vibrational modes. Considering predissociation mechanism, on the other hand, theoretical studies on the potential energy surfaces in the excited electronic states as well as studies of photodissociation dynamics at different photon energies should be required.

Acknowledgements. This work was financially supported by Korea Science and Engineering Foundation.

References

1. Turner, B. E.; Kislyakov, A. G.; Liszt, H. S.; Kaifu, N. *Astrophys. J.* **1975**, *201*, 149.
2. Ichikawa, K.; Hamada, Y.; Sugawara, Y.; Tsuboi, A. *Chem. Phys.* **1982**, *72*, 301.
3. Brown, R. D.; Godfrey, P. D.; Kleiboemer, B. *J. Mol. Spectrosc.* **1985**, *114*, 257.
4. Birk, M.; Winneweisser, M. *Chem. Phys. Lett.* **1986**, *123*, 382.
5. Birk, M.; Winneweisser, M. *J. Mol. Spectrosc.* **1993**, *159*, 69.
6. Moruzzi, G.; Jabs, W.; Winneweisser, B. P.; Winneweisser, M. *J. Mol. Spectrosc.* **1998**, *190*, 353.
7. Jabs, W.; Winneweisser, M.; Belov, S. P.; Lewen, F.; Maiwald, F.; Winneweisser, G. *Mol. Phys.* **1999**, *97*, 213.

8. Hartmann, J.; Nawroth, T.; Dose, K. *Origins Life* **1984**, *14*, 213.
 9. Tordini, F.; Bencini, A.; Bruschi, M.; De Gioia, L.; Zampella, G.; Fantucci, P. *J. Phys. Chem. A* **2003**, *107*, 1188.
 10. Duvernay, F.; Chiavassa, T.; Borget, F.; Aycard, J. P. *J. Phys. Chem. A* **2005**, *109*, 603.
 11. Eng, R.; Filseth, S. V.; Carrington, T.; Dugan, H.; Sadowski, C. M. *Chem. Phys. Lett.* **1988**, *146*, 96.
 12. Park, J.; Yu, C. F.; Bersohn, R. *Chem. Phys.* **1989**, *134*, 421.
 13. North, S. W.; Hall, G. E. *Chem. Phys. Lett.* **1996**, *263*, 148.
 14. Oh, C. Y.; Shin, S. K.; Kim, H. L.; Park, C. R. *Chem. Phys. Lett.* **2001**, *342*, 27.
 15. Li, R.; Derecskei-Kovacs, A.; North, S. W. *Chem. Phys.* **2000**, *254*, 309.
 16. Oh, C. Y.; Park, T. J.; Kim, H. L. *Bull. Korean Chem. Soc.* **2005**, *26*, 1177.
 17. Oh, C. Y.; Shin, S. K.; Kim, H. L.; Park, C. R. *J. Phys. Chem. A* **2003**, *107*, 4333.
 18. Kang, T. Y.; Choi, H. S.; Shin, S. K.; Kim, H. L. *J. Phys. Chem. A* **2004**, *108*, 8027.
 19. Engelman Jr., R. *J. Mol. Spectrosc.* **1974**, *49*, 106.
 20. Herzberg, G. *Molecular Spectra and Molecular Structure: I Spectra of Diatomic Molecules*; Van Nostrand Reinhold: New York, 1950.
 21. Nicholls, R. W. *J. Res. Nat. Bur. Stand. Sec. C* **1964**, *68A*, 75.
 22. Salley, D. J.; Gray, J. B. *J. Am. Chem. Soc.* **1951**, *73*, 5925.
 23. DeWit, H. G. M.; DeKruif, C. G.; Van Miltenberg, J. C. *J. Chem. Thermodyn.* **1983**, *15*, 891.
 24. Tuck, A. F. *J. Chem. Soc. Faraday Trans. II* **1977**, *73*, 689.
 25. Frisch, M. J. *et al. Gaussian 98*; Gaussian Inc.: Pittsburgh, PA, 1998.
 26. Zamir, E.; Levin, R. D. *Chem. Phys.* **1980**, *52*, 253.
 27. Levin, R.; Bernstein, R. B. *Molecular Reaction Dynamics and Chemical Reactivity*; Oxford University Press: New York, 1987.
 28. Herzberg, G. *Molecular Spectra and Molecular Structure: III Electronic Spectra and Electronic Structure of Polyatomic Molecules*; Van Nostrand Reinhold: New York, 1966.
-